Membrane Cholesterol Is a Biomechanical Regulator of Neutrophil Adhesion

Hana Oh, Emile R. Mohler III, Aiwei Tian, Tobias Baumgart, Scott L. Diamond

Objective—The purpose of this study was to evaluate the role of membrane cholesterol on human neutrophil and HL-60 biomechanics, capture, rolling, and arrest to P-selectin– or IL-1–activated endothelium.

Methods and Results—Methyl-β-cyclodextrin (MβCD) removed up to 73% and 45% of membrane cholesterol from HL-60 cells and neutrophils, whereas MβCD/cholesterol complexes resulted in maximum enrichment of 65% and 40%, respectively, above control levels. Cells were perfused at a venous wall shear rate of 100 s^{-1} over adherent P-selectin–coated 1-μm diameter beads, uncoated 10-μm diameter beads, P-selectin–coated surfaces, or activated endothelium. Elevated cholesterol enhanced capture efficiency to 1-μm beads and increased membrane tether growth rate by 1.5- to 2-fold, whereas cholesterol depletion greatly reduced tether formation. Elevated cholesterol levels increased tether lifetime by 17% in neutrophils and adhesion lifetime by 63% in HL-60 cells. Deformation of cholesterol-enriched neutrophils increased the contact time with 10-μm beads by 32% and the contact area by 7-fold. On both P-selectin surfaces and endothelial-cell monolayers, cholesterol-enriched neutrophils rolled more slowly, more stably, and were more likely to firmly arrest. Cholesterol depletion resulted in opposite effects.

Conclusions—Increasing membrane cholesterol enhanced membrane tether formation and whole cell deformability, contributing to slower, more stable rolling on P-selectin and increased firm arrest on activated endothelium. **(*Arterioscler Thromb Vasc Biol*. 2009;29:1290-1297.)**

Key Words: neutrophils ■ cholesterol ■ cell adhesion ■ endothelium ■ membrane ■ inflammation

Although macrophages are widely accepted as primary modulators of atherosclerosis, neutrophils may also contribute.[1,2] Neutrophils are prevalent in ruptured plaques,[3] and activated neutrophils secrete proteinases that may promote plaque rupture. In pathological states of high cholesterol levels or impaired cellular cholesterol processing, high membrane cholesterol levels in neutrophils may impact vascular disease via biomechanical or biological mechanisms. Leukocyte adhesion and emigration are elevated in mice placed on a high-cholesterol diet.[4] Neutrophils from HC (hypercholesterolemic) subjects produce more superoxide and display increased adhesion to human umbilical vein endothelial cells.[5,6]

Cholesterol-associated changes in cellular biomechanics have been investigated in several cell types. In endothelial cells, cholesterol depletion increases membrane stiffness[7] and decreases lateral lipid diffusion.[8] Lower cholesterol levels result in decreased protein mobility in the plasmalemma of skin fibroblasts.[9] Similarly, in leukocytes, cholesterol depletion decreases deformability during aspiration,[10,11] suppresses fMLP-induced ruffling and polarization,[12] and reduces actin polymerization.[13] In contrast, cholesterol enrichment increases membrane stiffness in pure lipid.[14] Whereas Abbal et al found that cholesterol extraction reduced T-cell rolling,[15] others did not detect changes in rolling behavior from cholesterol extraction.[16]

Responses to cholesterol enrichment or depletion may vary depending on each cell type and are difficult to predict without direct measurement. Also, membrane mechanics and whole cell mechanics, although interrelated, are independent entities. Neutrophil mechanics and membrane tether dynamics can affect neutrophil rolling,[17–19] and various agents such as ethanol can alter these processes.[20] The effect of cholesterol on neutrophil adhesion remains understudied because most cholesterol enrichment protocols involve overnight incubation which is not feasible with neutrophils.[21] We modified existing protocols to increase cholesterol content within 30 minutes in neutrophils and HL-60 cells, a well-established model system for neutrophils,[22] using MβCD/cholesterol complexes at defined molar ratios. We deployed a methodology to enrich or deplete cholesterol concentration and examined the effect on neutrophil and HL-60 cell mechanics during capture, membrane tether extension, rolling, and adhesion at venous shear rates to P-selectin or activated endothelium.

Methods

Additional descriptions of Materials, Cell Culture, Whole-Cell Deformation Assay Parameters, Fluorescence Recovery After Photo-

Received October 18, 2008; revision accepted April 23, 2009.

From the Department of Chemical and Biomolecular Engineering, Institute for Medicine and Engineering (H.O., S.L.D.), the Department of Medicine (E.R.M.), and the Department of Chemistry (A.T., T.B.), University of Pennsylvania, Philadelphia.

Correspondence to Scott L. Diamond, 1024 Vagelos Research Laboratory, 3340 Smith Walk, Philadelphia, PA 19104. E-mail sld@seas.upenn.edu

bleaching (FRAP), and Flow Cytometry are available as supplemental materials (available online at http://atvb.ahajournals.org).

Membrane Cholesterol Depletion and Enrichment

MβCD solution was prepared by dissolving MβCD in RPMI1640 medium without phenol red and without serum. For cholesterol depletion, cells were incubated with MβCD solution at varying concentrations (5 to 20 mmol/L) for 30 minutes. Cholesterol enrichment was performed by treatment with MβCD/cholesterol complexes as described previously.[23] Briefly, cholesterol stock solution was added to a glass tube, the solvent was evaporated, and 5 mmol/L MβCD was added to the dried cholesterol.

The tube was sonicated for 10 minutes and placed in a shaking incubator overnight at 37°C. The ratio of MβCD:cholesterol was varied to determine the equilibrium and saturation ratios for HL-60 cells and neutrophils (See Results). The amount of cholesterol was quantified using the Amplex Red assay (Molecular Probes) as described in the supplemental materials.

Neutrophil-Microbead Collision Assay

The neutrophil-microbead collision assay was used to probe interactions between neutrophils under flow and a small point source of P-selection. Polystyrene 1.05-μm-diamter microspheres coated with Protein A (Bangs Labs) were labeled with recombinant human CD62P/Fc chimera P-selectin with IgG1 Fc region (R&D Systems) as previously described.[24] Flow chambers were assembled using rectangular glass capillaries (Vitrocom) with a dimension of 0.2×2.0×70 mm and a wall thickness of 0.15 mm. The P-selectin–coated beads (1.7×10^4 P-selectin/bead) were incubated for attachment to glass capillary flow chambers, rinsed, and blocked with HBSS with 2% HSA. Because anti–PSGL-1, calcium-free buffer, or P-selectin–free beads all result in zero detectable adhesion events, this assay probes the specific interactions with P-selectin.

Whole-Cell Deformation Assay

Flow chambers were assembled as described above. The 10-μm-diameter Polystyrene "Polybeads" (Polisciences) were incubated for 2 hours at 4°C with 200 μg/mL fibrinogen to facilitate attachment to the chamber. Fibrinogen does not cause β2-integrin–mediated adhesion in this assay.[24] The 10-μm beads in HBSS with 2% HSA and were perfused into the capillary flow chambers for attachment to the bottom overnight at room temperature. The chambers were washed and blocked HBSS with 2% HSA.

P-Selectin–Coated Surface Perfusion Assay

To prepare P-selectin–coated surfaces, flow chambers were incubated with affinity-purified human P-selectin (R&D Systems) in Ca^{2+}- and Mg^{2+}-free HBSS at 1 μg/mL final concentration for at least 3 hours at room temperature. Excess unbound protein was removed by perfusing HBSS through the chamber for 30 minutes. The final P-selectin site density was previously determined as ≈10 sites/μm^2[18] at identical coating conditions.

Endothelial Cell Parallel Plate Flow Chamber

Confluent monolayers of human aortic endothelial cells (HAECs) on glass slides were exposed to steady laminar shear stress in parallel plate flow chambers attached to flow loops for media recirculation (15 mL) in a 37°C incubator as previously described.[25] HAECs were treated with Interleukin-1 (IL-1; BioLegend) for 5 hours for activation under continuous flow conditions.[26]

Imaging and Video Analysis

Microcapillary flow chambers were observed with an inverted microscope (Zeiss Axiovert 135) using differential interference contrast (DIC) with a 63× oil immersion objective (Zeiss, Plan-Apochromate) and high-illuminating aperture with automatic-aplanatic condenser (Numeric Aperture 1.4). Data were recorded and analyzed (Scion Image and ImageJ) to obtain rolling length, velocity, and firm arrest data as previously described[20] (see the supplemental materials).

The following definitions were used (as defined in[20]). "Adhesive interactions" refer to collisions with visible pauses in neutrophil motion lasting for at least 1 frame during frame-by-frame analysis. "Adhesive tether-forming neutrophils" are neutrophils that translate in the direction of flow at a velocity below the hydrodynamic stream velocity, form a tether, and are rapidly released. The following parameters were obtained from the neutrophil-bead collision assay: "adhesion efficiency" (ε), which is the number of collisions resulting in an adhesive interaction divided by the total number of collisions; "membrane tethering fraction" (f), which refers to the ratio of tether-forming events to the total number of adhesive interactions; "lifetimes" are the duration of adhesive and tether-forming interactions; "tether lengths" are the distance from the center of the adhesive bead to the lagging edge of the neutrophil as measured by the ImageJ software. The "mean tether growth velocity" (v_t) was calculated by dividing the tether length by the tether lifetime. Parameters for the whole-cell deformation assay are explained in the supplemental materials.

Cells rolling on P-selectin surfaces were analyzed using the following parameters: average rolling velocity, which is the total distance traveled by a rolling cell divided by the time; variance of velocity, which indicates the fluctuations of cell velocity during cell rolling behavior; flux of rolling cells, the ratio of rolling cells to total number of flowing cells in a given field of view (FOV), which was about 0.01 mm^2 in this assay; and fraction arrested, which is the ratio of to all flowing cells in a field of view.

For the neutrophil-HAEC assay on flow chambers, the following definitions were used: "firmly arrested neutrophils" refer to cells that remain motionless during time of observation in FOV (10 s); "rolling distance" is the distance between the point of first adhesive contact between a neutrophil and the endothelial cells and the point at which the neutrophil stops rolling and remains stationary.

Results

Cholesterol Depletion and Enrichment in HL-60 and Neutrophils

We measured the baseline cholesterol content of HL-60 cells and neutrophils as 3.5±0.5 nmol/10^6 cells and 1.31±0.23 nmol/10^6 cells, respectively. To deplete cells of membrane cholesterol, we incubated cells with MβCD for 30 minutes and verified that this incubation time did not cause significant changes in morphology or viability in either cell type. With fixed incubation time, we varied only the MβCD concentration from 5 mmol/L to 20 mmol/L to control the extent of cholesterol extraction (Figure 1A). At each MβCD concentration tested, the same concentration resulted in a larger decrease in cholesterol levels in HL-60 cells than in neutrophils. A 10 mmol/L MβCD treatment resulted in a 60% reduction in HL-60 membrane cholesterol levels, compared to 34% in neutrophils. As specific doses, MβCD had distinct effects on the two cell types, as expected.[27]

The use of MβCD/cholesterol complexes to enrich cell membranes with cholesterol requires attention to the equilibrium and saturation ratios deployed for each cell type.[27] These ratios have not been established for HL-60 or neutrophils. We determined the optimal MβCD:cholesterol ratio for neutrophils and HL-60 (Figure 1B). The enrichment response was significantly different in neutrophils compared to HL-60 cells. While a ratio of 8:1 resulted in 65% enrichment in HL-60 cells, the same ratio had no effect on the cholesterol content of neutrophils. Increasing the ratio to 4:1 yielded 65% enrichment in HL-60 cells, compared to 40% enrichment in

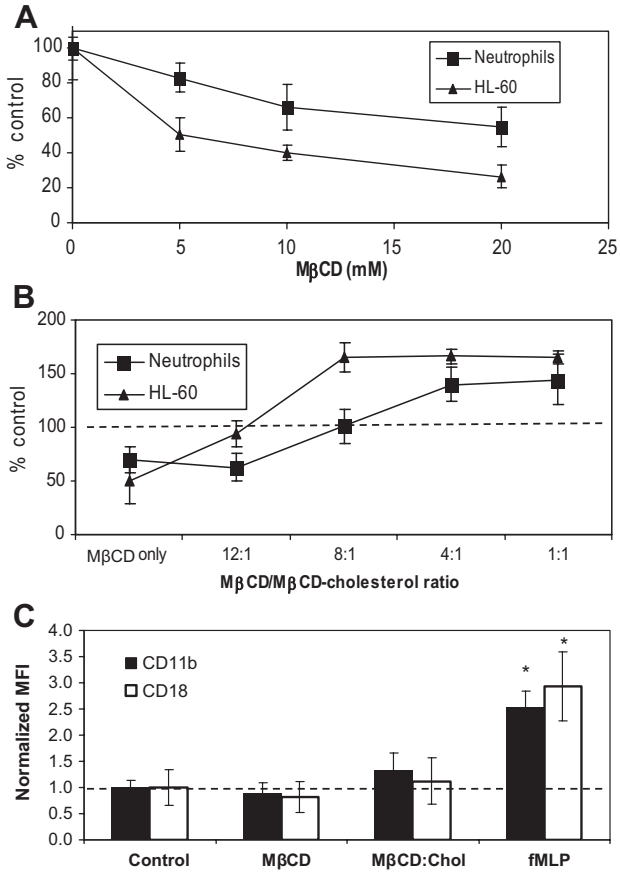

Figure 1. Cholesterol depletion and enrichment of neutrophils and HL-60 cells and the effect on surface integrin expression. Cells were cholesterol-depleted by incubation with MβCD (A) or cholesterol-enriched with MβCD-cholesterol complexes (B). Cholesterol content after each treatment was normalized to control levels. N=4 donors. Mean fluorescence intensity (MFI) of FITC-conjugated CD11b and CD18 were normalized to control levels for each (C). N=3 donors.

neutrophils. The saturation ratios were different for the two cell types: 8:1 for HL-60 and 4:1 for neutrophils. The maximum percent increase was 65% in HL-60 and 43% in neutrophils.

We measured the levels of integrin expression on surfaces of cholesterol-depleted or enriched neutrophils, and compared them to expression levels of fMLP-stimulated neutrophils. As expected, fMLP stimulation more than doubled surface CD11b and CD18 levels, whereas changes in membrane cholesterol levels did not cause neutrophils to activate, because expression of MAC-1 subunits remained unchanged from control levels (Figure 1C).

We performed adhesion and rolling assays after increasing the cholesterol content by 65% in HL-60 cells and 40% in neutrophils. These levels are similar to the concentrations we measured in neutrophils obtained from hypercholesterolemic (HC) patients (plasma cholesterol >300 mg/dL), which we found to be 73% higher than concentrations found in normal subjects (2.26 ± 0.09 nmol/10^6 cells in HC patients, N=4, compared to 1.31 ± 0.23 nmol/10^6, N=5; $P<0.01$). Seres et al have previously reported an 89% increase in cholesterol concentration in neutrophils from HC patients.[28]

Membrane Cholesterol Regulates P-Selectin/PSGL-1–Mediated Adhesion

To study the adhesion and tethering response of HL-60 cells and neutrophils, we analyzed collisions with P-selectin–coated 1-μm diameter beads using high-speed high-resolution videomicroscopy to obtain adhesion and tethering parameters. In both cell types tested at 100 s^{-1}, cholesterol enrichment increased adhesion efficiency, tethering fraction, length of tethers, and tether growth velocity (Table 1). Cholesterol enrichment resulted in a significant increase in the membrane tether length and growth rate. The tether growth rate more than doubled in HL-60 cells and increased by a factor of 1.8 in neutrophils. Tether length increased by a factor of 1.6 in HL-60 cells and doubled in neutrophils. Cholesterol depletion decreased the adhesion efficiency of HL-60 cells, whereas it resulted in a slight increase for neutrophils. Adhesion lifetimes of HL-60 cells (± tethers) were enhanced with increasing concentrations of cholesterol, whereas the adhesion lifetimes of neutrophils were unaffected. Interestingly, the tether lifetimes of neutrophils were enhanced with increasing levels of cholesterol, whereas that of HL-60 cells were unaffected. The tethering fraction of control HL-60 cells was much lower (0.29 compared to 0.63 for neutrophils) and was abolished in cholesterol-depleted HL-60 cells (Table 1), indicating that the ability to resist tether extraction in HL-60 cells was greater.

Membrane Tether Growth Is Enhanced With Increasing Cholesterol

Using frame-by-frame analysis of neutrophil tether extraction, we obtained instantaneous tether lengths for 10 choles-

Table 1. Effect of Cholesterol Depletion and Enrichment on Adhesion of Neutrophils and HL-60 Cells to P-Selectin–Coated Beads at 100 s^{-1}

	Neutrophils			HL-60 Cells		
	30% Depletion (44/378)	Control (35/435)	40% Enrichment (42/291)	50% Depletion (6/402)	Control (17/534)	65% Enrichment (19/357)
Adhesion efficiency	0.12±0.05 *	0.08±0.05	0.14±0.08 *	0.015±0.006*	0.032±0.012	0.053±0.013*
Adhesion lifetime, s	0.31±0.12	0.30±0.11	0.36±0.10	0.25±0.21	0.27±0.22	0.44±0.19**
Tether fraction	0.45±0.08*	0.63±0.16	0.74±0.14*	0*	0.29±0.12	0.37±0.15**
Tether length, μm	0.67±0.35*	2.50±0.54	5.30±2.10*	0*	4.13±2.12	6.40±3.40**
Tether lifetime, s	0.38±0.12*	0.53±0.21	0.62±0.23*	0*	0.64±0.30	0.42±0.19
Tether growth velocity, μm/s	1.76±1.08*	4.72±2.13	8.55±4.64*	0*	6.4±2.5	14.9±8.3*

*$P<0.01$, **$P<0.05$, untreated vs MβCD- or MβCD-cholesterol-treated. (Adhesive events/total interactions.)

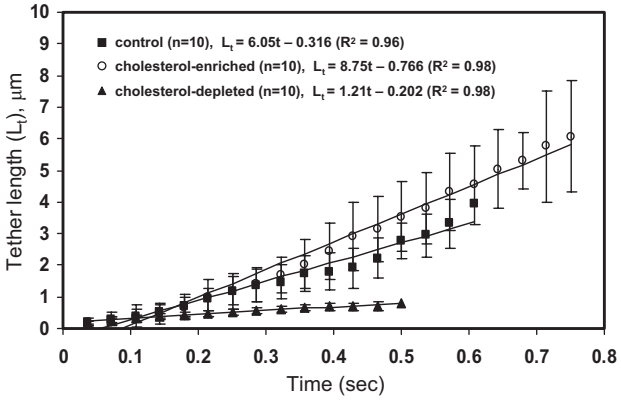

Figure 2. Instantaneous tether growth of cholesterol-depleted, control, and cholesterol-enriched neutrophils. Tether length was measured frame-by-frame during neutrophil-bead adhesion for 10 representative tethers under each condition. The averages and the linear fit are compared. Mean±SD. N=3 donors.

terol-depleted, cholesterol-enriched, and untreated neutrophils (Figure 2). The length, lifetime, and growth rate of tethers all increased with higher cholesterol content. The average of all 10 tethers under each condition reveals that tether growth is highly linear and that tethers of cholesterol-depleted cells grow at a much slower rate compared to control or cholesterol-enriched cells (Figure 2). These results suggested faster lipid flow as the membrane stretched out into tethers.

We also performed fluorescence recovery after photobleaching (FRAP) measurements of lipid diffusivity in a pulled tether. We found that cholesterol loading caused a statistically significant increase of 1.38-fold (P=0.04) in lipid diffusivity in the neutrophil tether (0.147±0.022 $\mu m^2/s$ control versus 0.223±0.053 $\mu m^2/s$ with cholesterol; n=8 tethers).

Cholesterol Increases Whole Cell Deformability

To test the hypothesis that cholesterol alters whole cell deformability, we perfused cholesterol-depleted or enriched cells into glass capillary flow chambers which presented adherent 10-μm diameter beads (no P-selectin). Because the beads were comparable to neutrophils in size, the cell-bead collisions enabled us to study cell deformation at the whole cell scale. Compared with untreated neutrophils colliding with the beads (Figure 3A), cells with increased cholesterol concentration in the membrane appeared more deformed during collision (Figure 3B). To further quantify the changes in deformation, we measured the distance between the center of the cell and the center of the bead, and subtracted the value for rigid spheres to obtain R (Figure 3C, inset), which equals 0 for 2 rigid spheres.

Figure 3C shows that cells without any treatment did not deviate significantly from the R=0 centerline, with a maximum deviation of R=−0.2 μm (Table 2). Because the average lengths of microvilli on the neutrophil surface are also about 0.2 to 0.3 μm,[29] this value likely reflects compression of microvilli rather than global cellular deformation. Cholesterol-enriched cells, however, displayed a much more significant degree of compliance, as shown in Figure 3B and 3C. The value of R for cholesterol-treated cells continued to

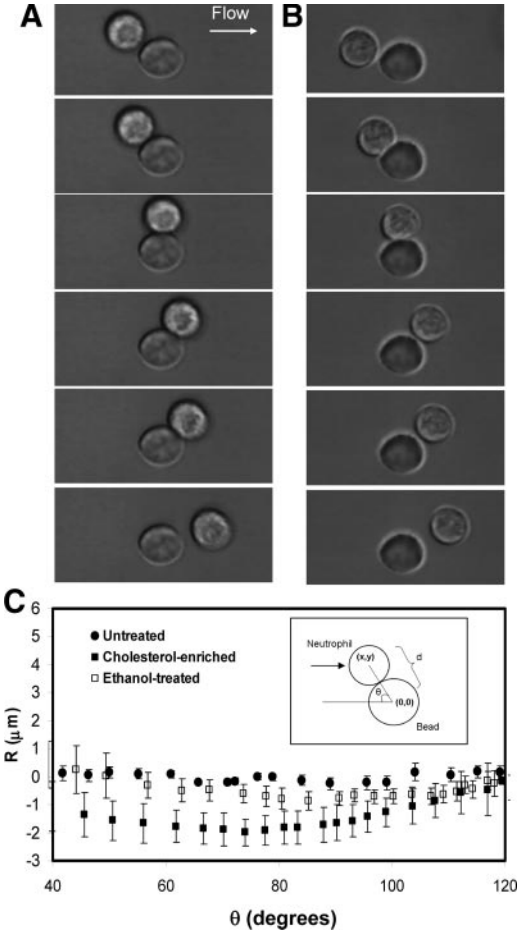

Figure 3. Neutrophil whole-cell deformation by centroid tracking. Image sequences were obtained during neutrophil collision with 10-μm-diameter beads at 240 fps videomicroscopy for untreated neutrophils (A) and cholesterol-enriched neutrophils (B). The distance between the centroids of the cell and the bead, R, was tracked (C). Mean±SD of 10 cells under each condition.

decrease as θ increased, which shows that the deformation continued to increase throughout the collision. Maximum deformation was reached at a contact angle of 74 degrees, after which deformation continuously decreased. For comparison, we observed the deformability of cells treated with 0.3% ethanol (Figure 3C), which has been previously shown to significantly alter membrane and tether mechanics.[20] Ethanol-treated cells deformed during collision as well, but the magnitude was substantially smaller than cholesterol-treated cells (R=−0.8±0.04 μm, compared to R=−1.8±0.03 μm for cholesterol-treated cells). This supports a view that the mechanics of the membrane and tether do not predict whole cellular deformability and that these characteristics must be examined separately.

We measured the length of contact time during collisions between the cells and the beads using high-speed imaging (240 fps). The duration of contact time was 32% longer in cholesterol-treated cells (Table 2). Becuase the large beads used in this study did not present P-selectin for the molecules on the cell surface to bind (and no adhesion was detected as indicated by delayed release), the increase in contact time can

Table 2. Neutrophil Deformation During Collisions With Adherent 10-μm Diameter Beads (Uncoated) at 100 s^{-1}

	Neutrophils (No Treatment) (n=21 int)	Neutrophils+Ethanol (n=24 int)	Neutrophils+Cholesterol (n=25 int)
Average contact lifetime, s	0.17±0.09	0.19±0.08	0.25±0.10*
Max deformation, minimum *R*	−0.2±0.03 μm	−0.8±0.04 μm*	−1.8±0.03 μm*
Max contact area	5 μm^2	18 μm^2	35 μm^2
	(1×)	(3×)	(7×)

*$P<0.01$ compared to control. n=int indicates number of interactions.

be attributed primarily to changes in the inherent compliance of the cell, which provides direct evidence that cholesterol affects cells at submembrane structures and whole cell level.

Based on the changes in *R* values, we also calculated the maximum contact area between the cell and the bead during collision and found that the area increased 3-fold for ethanol-treated cells and 7-fold for cholesterol-enriched cells (Table 2). In addition to the prolonged contact time, the increase in contact area would markedly increase the chances of bond formation when cells interact with selectin- or integrin-expressing surfaces.

Neutrophils With Higher Cholesterol Levels Roll More Slowly and Uniformly on P-Selectin

To test whether enhanced deformability and tether formation rate would alter neutrophil rolling, we perfused cells with different membrane cholesterol levels over P-selectin–coated surfaces. Rolling velocity decreased with increasing cholesterol concentration. The average velocity was 11.2 μm/s for cholesterol-depleted neutrophils, but 4.5 μm/s for cholesterol-enriched cells, both of which differed significantly from untreated cells (Table 3). Cells with higher membrane cholesterol content also rolled more uniformly on P-selectin–coated surface. The variance in rolling velocity was 5.2 $(\mu m/s)^2$ for cholesterol-enriched cells, compared to 15.2 $(\mu m/s)^2$ for depleted cells. Although the flux of rolling cells was unaffected, the fraction of cells converting to firm arrest increased from 35.3 cells/FOV for untreated cells to 41.1 cells/FOV for cholesterol-treated cells ($P<0.01$) (Table 3).

In tests with neutrophils from HC patients (N=4, average age: 64±3) free of statin therapy, Table 3 demonstrates that HC neutrophils rolled more slowly ($P<0.01$) and with less variance ($P<0.01$) on P-selectin–coated surfaces than neutrophils from healthy donors. Additionally, the rolling flux on P-selectin coated surfaces (cells per unit area) increased by 19% ($P<0.01$) and conversion to firm arrest increased by 22% ($P<0.01$) compared to neutrophils from nonage matched healthy donors (average age: 30).

Rolling and Arrest on Activated Endothelium

HAEC monolayers were treated with IL-1 for 5 hours before a neutrophil adhesion assay in a parallel-plate flow chamber at wall shear rate of 100 s^{-1}. We have previously shown that without IL-1 stimulation, neutrophils displayed little rolling or firm arrest[20] and shear exposure alone for 5 hours alone did not promote subsequent adhesion tested at 100 s^{-1}.[26] Cholesterol-enriched neutrophils rolled more slowly on IL-1–activated HAEC monolayers, compared to untreated cells or cholesterol-depleted cells, as they did on P-selectin. Cells with higher cholesterol content were more likely to roll and convert to firm arrest compared to control cells. The flux of rolling cells increased from a control value of 41.1 cells/FOV to 52.7 cells/FOV, and the percentage of firmly arrested cells in a given FOV increased from 33.2% to 43.6% with cholesterol enrichment ($P<0.01$). Cells with reduced cholesterol levels exhibited the opposite behavior, as flux decreased to 31.9 cells/FOV and firm arrest percentage decreased to 22.7% (Table 3).

Discussion

Elevated cholesterol enhanced capture efficiency to 1-μm beads and increased membrane tether growth rate by 1.5- to 2-fold, whereas cholesterol depletion greatly reduced tether formation. The increased cell deformability and faster membrane tether growth was consistent with the slower rolling and increased probability of firm arrest we observed for cholesterol-enriched cells (Table 3). On both P-selectin surfaces and endothelial-cell monolayers, cholesterol-enriched neutrophils rolled more slowly, more stably, and were more

Table 3. Neutrophils Rolling on P-Selectin–Coated Surface and Activated HAEC Monolayer

	P-Selectin Surface			IL-1/HAEC Monolayer			HC Neutrophils on P-Selectin Surface (N=4)
	30% Depletion (n=31)	Control (n=37)	40% Enrichment (n=41)	30% Depletion (n=45)	Control (n=51)	40% Enrichment (n=63)	
Average rolling velocity, μm/s	11.2±2.4*	8.9±1.3	4.5±0.9*	12.1±4.1	10.9±3.3	6.1±3.7*	6.8±1.2*
Variance of rolling velocity, $\mu m/s^2$	15.2±3.5*	12.1±2.4	5.2±2.1*	8.9±2.1	9.2±1.6	8.7±2.6	10.3±1.2*
Flux of rolling cells, # cells/FOV	10.5±3.5	12.8±4.2	11.7±3.1	31.9±8.1*	41.1±11.2	52.7±7.2*	15.2±4.2*
Percent arrested/FOV	33.6±8.7	35.4±4.1	41.1±5.1*	22.7±5.2*	33.2±5.0	43.6±4.8*	43.1±3.5*

All measurements at 100 s^{-1}.

*$P<0.01$ compared to control; FOV=≈0.01 mm^2; n indicates number of interactions; N, donors.

likely to firmly arrest. Cholesterol depletion resulted in opposite effects.

More than 90% of cellular cholesterol is found in the plasma membrane.[30,31] Thus, we examined tether extrusion from cells under flow which provides insight to the lipid flow from the membrane as well as the adhesion strength between the bilayer and the underlying cytoskeleton, with important implications on bond loading and neutrophil rolling dynamics as studied previously.[18] We have found that with increasing cholesterol content, a higher fraction of both neutrophils and HL-60 pulled tethers (Table 1). Also, the 1.5- to 2-fold increase in average tether length suggests that the cholesterol-enriched membrane is more likely to dissociate from the cytoskeleton to form longer tethers, whereas the increase in the growth velocity of the tethers indicate increased fluidity.

A mechanical mechanism is well supported by the experimental data. As previously shown,[18,24] longer tethers reduce the force loading on the bonds by changing the angle of the mechanical lever arm,[17] thus resulting in a longer lifetime of bonds. To help verify the mechanical-level mechanism underpinning the observation of enhanced tether growth with elevated cholesterol, we have taken FRAP measurements of lipid diffusivity in a pulled tether. We found that cholesterol loading increased lipid diffusivity in the tether by 1.38-fold ($P=0.04$). By lowering the viscosity, the elevated cholesterol makes it easier to pull a tether at a given mechanical loading, which leads to faster growing and longer tethers (Figure 2) that reduced the lever arm and consequently shielded the bond from force loading, thereby lengthening the bond lifetimes (Table 1) and stabilizing rolling (Table 3).

Cholesterol-enriched membrane fluidity has been previously measured using fluorescence polarization (FP) to probe the molecular rotational diffusivity of fluorescent lipids. Typically, cholesterol will reduce "membrane fluidity,"[28,32] but molecular membrane fluidity is not predictive of translational diffusivity measured by FRAP. In contrast, others have shown an increase in fluidity with cholesterol loading.[8,33,34] The FP probe localizes in the membrane whereas FRAP samples larger areas of membrane that may have heterogeneity. Cholesterol effects on the membrane-cytoskeletal linkage, which would also alter mechanically-driven lipid flow into tethers, would not be predicted by FP. Changes in cell shape (Figure 3) indicate that cholesterol effects on the cytoskeleton result in more compliant cells and faster tether growth. Clearly, the effect of membrane cholesterol varies greatly from one cell type to another and depend on experimental technique which measures lipid mobility on length scales of nanometer (FP), micron (FRAP), or several microns (tether pulling and deformation).

We also examined the effect of varying cholesterol levels on whole cell deformation. Previous studies have suggested that the mechanism of actin polymerization may be separate from the mechanism governing pseudopod formation and viscoelastic recovery.[35] During collision with 10-μm diameter beads, cells with elevated cholesterol deformed to an extent that the distance between the centroids of the cell and the bead decreased by 1.8 μm compared to 2 hard spheres during collision. The magnitude of the effect of cholesterol on cell rigidity becomes more apparent when compared to the effect of ethanol (0.3% by vol.), which also influences tether mechanics and rolling behavior.[20]

Deformability of neutrophils at the whole-cell level has several physiological implications. In vivo, leukocytes flatten against the endothelial wall to reach aspect ratios of up to 1.4.[36] Mechanosensing abilities of compliant neutrophils have been suggested from studies of mechanical deformation into narrow channels,[35] whereas large-scale deformation of neutrophils has been shown to lead to activation.[37] According to computational studies, cellular deformation decreases the drag on the cell and may help account for a plateau of rolling velocity with increasing shear rate.[38] We conclude that cholesterol-induced changes in membrane tether growth and cell deformability are likely to contribute toward enhanced adhesion and firm arrest that have been observed in vivo in high-cholesterol environment.[4,6]

The increased deformability after cholesterol enrichment led to a 7-fold increase in contact area between cells and 10-micron beads, as well as a 32% increase in contact time (Table 2), both of which may favor increased bonding. In fact, cholesterol enrichment stabilized rolling behavior, decreased rolling velocity, and increased firm arrest (Table 3).

Cholesterol enrichment and depletion are expected to have a number of differing effects on neutrophils and neutrophil signaling beyond the direct effects of changing membrane mechanics, which in itself is a complex effect that impacts bonding dynamics with P-selectin. The prominent effect of cholesterol on both tether mechanics and cellular rigidity suggests a link between cholesterol and the actin cytoskeleton.[8,9] Because cholesterol removal by MβCD has been shown to inhibit polymerization[13] and disruption of actin cytoskeleton has been shown to interfere with intrinsic selectin adhesiveness,[16] it is also possible that cholesterol effects on the actin network alter the mobility of adhesion molecules in the membrane which affects their binding ability. Also, disruption of the interaction between PSGL-1 and the actin cytoskeleton has been previously shown to reduce adhesion and rolling on P-selectin.[39]

We observed faster P-selectin–mediated rolling and reduced adhesion for cholesterol-depleted cells, in contrast to cholesterol-enriched cells, which confirms previous observations[10] and computational modeling studies[40] of faster rolling of stiffer cells. It is also consistent with prior observation that faster rolling attenuates activation of integrin-mediated arrest,[41] and that cholesterol extraction disrupts integrin-mediated adhesive process.[16]

The effect of membrane tethers on rolling stability (ie, reduced variance, Table 3) has been well established.[11] Because rolling has been shown to be unaffected by the intracellular domain of PSGL-1,[42] we conclude that the reduction in variance of rolling velocity by cholesterol loading or with neutrophils from HC patients was attributable to enhanced membrane tether growth (Table 1) and increased deformability with a consequent increase in contact area during rolling (Figure 3). A functional consequence of altered rolling dynamics, namely increased firm arrest, was detected with neutrophils from HC patients.

Inspection of Table 3 indicates that by all measures the neutrophils from HC patients are strikingly similar to choles-

terol-loaded neutrophils (from healthy donors) and strikingly dissimilar from cholesterol-depleted neutrophils. However, cholesterol depletion has complex biochemical effects on neutrophils, distinct from mechanical changes, that include ablation of caveolae and changes in calcium entry.[43] Still, the rolling flux and percent arrested on P-selectin surfaces were not statistically different for cholesterol depleted cells and control neutrophils (Table 3), however both these attributes were reduced (but not ablated) on IL-1–stimulated HAECs. These observations are consistent with cholesterol depletion causing a biomechanical change in rolling dynamics, but a biochemical change in signaling dynamics needed for firm arrest. PSGL-1–dependent signaling dynamics such as Syk-dependent activation of LFA-1[42] and subsequent conversion to firm arrest of neutrophils from HC patients or cholesterol-enriched neutrophils from healthy donors remains an important subject of future study. Furthermore, the cell softening in cholesterol-loaded cells (Figure 3) was likely a result of changes in whole cell mechanics that include cytoskeletal function.

Overall, our results show that elevated cholesterol levels yield a slower more stable rolling behavior, likely attributable to longer tethers with increased lifetime and increased whole cell deformability with increased contact area during rolling. Distinct from purely biochemical effects, membrane cholesterol is a biomechanical regulator of tether growth and whole-cell mechanics which, in turn, modulates neutrophil rolling and adhesion.

Sources of Funding

This study was supported by National Institutes of Health grants HL 56621 and HL 66565.

Disclosures

None.

References

1. VanderLaan PA, Reardon CA. Thematic review series: The immune system and atherogenesis. the unusual suspects: An overview of the minor leukocyte populations in atherosclerosis. *J Lipid Res*. 2005;46:829–838.
2. Madjid M, Awan I, Willerson JT, Casscells SW. Leukocyte count and coronary heart disease: Implications for risk assessment. *J Am Coll Cardiol*. 2004;44:1945–1956.
3. Naruko T, Ueda M, Haze K, van der Wal AC, van der Loos CM, Itoh A, Komatsu R, Ikura Y, Ogami M, Shimada Y, Ehara S, Yoshiyama M, Takeuchi K, Yoshikawa J, Becker AE. Neutrophil infiltration of culprit lesions in acute coronary syndromes. *Circulation*. 2002;106:2894–2900.
4. Petnehazy T, Stokes KY, Wood KC, Russell J, Granger DN. Role of blood cell-associated AT1 receptors in the microvascular responses to hypercholesterolemia. *Arterioscler Thromb Vasc Biol*. 2006;26:313–318.
5. Ludwig PW, Hunninghake DB, Hoidal JR. Increased leucocyte oxidative metabolism in hyperlipoproteinaemia. *Lancet*. 1982;2:348–350.
6. Sugano R, Matsuoka H, Haramaki N, Umei H, Murase E, Fukami K, Iida S, Ikeda H, Imaizumi T. Polymorphonuclear leukocytes may impair endothelial function: Results of crossover randomized study of lipid-lowering therapies. *Arterioscler Thromb Vasc Biol*. 2005;25:1262–1267.
7. Byfield FJ, Aranda-Espinoza H, Romanenko VG, Rothblat GH, Levitan I. Cholesterol depletion increases membrane stiffness of aortic endothelial cells. *Biophys J*. 2004;87:3336–3343.
8. Sun M, Northup N, Marga F, Huber T, Byfield FJ, Levitan I, Forgacs G. The effect of cellular cholesterol on membranecytoskeleton adhesion. *J Cell Sci*. 2007;120:2223–2231.
9. Kwik J, Boyle S, Fooksman D, Margolis L, Sheetz MP, Edidin M. Membrane cholesterol, lateral mobility, and the phosphatidylinositol 4,5-bisphosphate-dependent organization of cell actin. *Proc Natl Acad Sci U S A*. 2003;100:13964–13969.
10. Yago T, Leppanen A, Qiu H, Marcus WD, Nollert MU, Zhu C, Cummings RD, McEver RP. Distinct molecular and cellular contributions to stabilizing selectin-mediated rolling under flow. *J Cell Biol*. 2002;158:787–799.
11. Ramachandran V, Williams M, Yago T, Schmidtke DW, McEver RP. Dynamic alterations of membrane tethers stabilize leukocyte rolling on P-selectin. *Proc Natl Acad Sci U S A*. 2004;101:13519–13524.
12. Niggli V, Meszaros AV, Oppliger C, Tornay S. Impact of cholesterol depletion on shape changes, actin reorganization, and signal transduction in neutrophil-like HL-60 cells. *Exp Cell Res*. 2004;296:358–368.
13. Pierini LM, Eddy RJ, Fuortes M, Seveau S, Casulo C, Maxfield FR. Membrane lipid organization is critical for human neutrophil polarization. *J Biol Chem*. 2003;278:10831–10841.
14. Needham D, Nunn RS. Elastic-deformation and failure of lipid bilayer-membranes containing cholesterol. *Biophys J*. 1990;58:997–1009.
15. Abbal C, Lambelet M, Bertaggia D, Gerbex C, Martinez M, Arcaro A, Schapira M, Spertini O. Lipid raft adhesion receptors and syk regulate selectin-dependent rolling under flow conditions. *Blood*. 2006;108:3352–3359.
16. Dwir O, Grabovsky V, Pasvolsky R, Manevich E, Shamri R, Gutwein P, Feigelson SW, Altevogt P, Alon R. Membranal cholesterol is not required for L-selectin adhesiveness in primary lymphocytes but controls a chemokine-induced destabilization of L-selectin rolling adhesions. *J Immunol*. 2007;179:1030–1038.
17. Shao JY, Hochmuth RM. Mechanical anchoring strength of L-selectin, beta(2) integrins, and CD45 to neutrophil cytoskeleton and membrane. *Biophys J*. 1999;77:587–596.
18. Schmidtke DW, Diamond SL. Direct observation of membrane tethers formed during neutrophil attachment to platelets or P-selectin under physiological flow. *J Cell Biol*. 2000;149:719–730.
19. Kadash KE, Lawrence MB, Diamond SL. Neutrophil string formation: Hydrodynamic thresholding and cellular deformation during cell collisions. *Biophys J*. 2004;86:4030–4039.
20. Oh H, Diamond SL. Ethanol enhances neutrophil membrane tether growth and slows rolling on P-selectin but reduces capture from flow and firm arrest on IL-1-treated endothelium. *J Immunol*. 2008;181:2472–2482.
21. Christian AE, Haynes MP, Phillips MC, Rothblat GH. Use of cyclodextrins for manipulating cellular cholesterol content. *J Lipid Res*. 1997;38:2264–2272.
22. Hauert AB, Martinelli S, Marone C, Niggli V. Differentiated HL-60 cells are a valid model system for the analysis of human neutrophil migration and chemotaxis. *Int J Biochem Cell Biol*. 2002;34:838–854.
23. Levitan I, Christian AE, Tulenko TN, Rothblat GH. Membrane cholesterol content modulates activation of volume-regulated anion current in bovine endothelial cells. *J Gen Physiol*. 2000;115:405–416.
24. Edmondson KE, Denney WS, Diamond SL. Neutrophil-bead collision assay: Pharmacologically induced changes in membrane mechanics regulate the PSGL-1/P-selectin adhesion lifetime. *Biophys J*. 2005;89:3603–3614.
25. Diamond SL, Eskin SG, Mcintire LV. Fluid-flow stimulates tissue plasminogen-activator secretion by cultured human-endothelial cells. *Science*. 1989;243:1483–1485.
26. Ji JY, Jing H, Diamond SL. Hemodynamic regulation of inflammation at the endothelial-neutrophil interface. *Ann Biomed Eng*. 2008;36:586–595.
27. Zidovetzki R, Levitan I. Use of cyclodextrins to manipulate plasma membrane cholesterol content: Evidence, misconceptions and control strategies. *Biochimica Et Biophysica Acta-Biomembranes*. 2007;1768:1311–1324.
28. Seres I, Foris G, Pall D, Kosztaczky B, Paragh G Jr, Varga Z, Paragh G. Angiotensin II-induced oxidative burst is fluvastatin sensitive in neutrophils of patients with hypercholesterolemia. *Metabolism*. 2005;54:1147–1154.
29. Park EY, Smith MJ, Stropp ES, Snapp KR, DiVietro JA, Walker WF, Schmidtke DW, Diamond SL, Lawrence MB. Comparison of PSGL-1 microbead and neutrophil rolling: Microvillus elongation stabilizes P-selectin bond clusters. *Biophys J*. 2002;82:1835–1847.
30. Lange Y, Ramos BV. Analysis of the distribution of cholesterol in the intact cell. *J Biol Chem*. 1983;258:15130–15134.
31. Lange Y, Ye J, Rigney M, Steck TL. Regulation of endoplasmic reticulum cholesterol by plasma membrane cholesterol. *J Lipid Res*. 1999;40:2264–2270.
32. Goodwin JS, Drake KR, Remmert CL, Kenworthy AK. Ras diffusion is sensitive to plasma membrane viscosity. *Biophys J*. 2005;89:1398–1410.

33. Geoffrey M. Cooper, Robert E. Hausman. *The Cell: A Molecular Approach*. IV. Sunderland MA, ed. Washington, DC: ASM Press, Sinauer Associates; 2007.
34. Garzetti GG, Tranquilli AL, Cugini AM, Mazzanti L, Cester N, Romanini C. Altered lipid-composition, increased lipid-peroxidation, and altered fluidity of the membrane as evidence of platelet damage in preeclampsia. *Obstet Gynecol*. 1993;81:337–340.
35. Yap B, Kamm RD. Mechanical deformation of neutrophils into narrow channels induces pseudopod projection and changes in biomechanical properties. (vol 98, pg 1930, 2005). *J Appl Physiol*. 2007;102:1729–1731.
36. Damiano ER, Westheider J, Tozeren A, Ley K. Variation in the velocity, deformation, and adhesion energy density of leukocytes rolling within venules. *Circ Res*. 1996;79:1122–1130.
37. Evans E, Kukan B. Passive material behavior of granulocytes based on large deformation and recovery after deformation tests. *Blood*. 1984;64: 1028–1035.
38. Lei X, Lawrence MR, Dong C. Influence of cell deformation on leukocyte rolling adhesion in shear flow. *J Biomech Eng Trans ASME*. 1999;121:636–643.
39. Snapp KR, Heitzig CE, Kansas GS. Attachment of the PSGL-1 cytoplasmic domain to the actin cytoskeleton is essential for leukocyte rolling on P-selectin. *Blood*. 2002;99:4494–4502.
40. Jadhav S, Eggleton CD, Konstantopoulos K. A 3-D computational model predicts that cell deformation affects selectin-mediated leukocyte rolling. *Biophys J*. 2005;88:96–104.
41. Hafezi-Moghadam A, Thomas KL, Prorock AJ, Huo Y, Ley K. L-selectin shedding regulates leukocyte recruitment. *J Exp Med*. 2001;193: 863–872.
42. Miner JJ, Xia L, Yago T, Kappelmayer J, Liu Z, Klopocki AG, Shao B, McDaniel JM, Setiadi H, Schmidtke DW, McEver RP. Separable requirements for cytoplasmic domain of PSGL-1 in leukocyte rolling and signaling under flow. *Blood*. 2008;112:2035–2045.
43. Kannan KB, Barlos D, Hauser CJ. Free cholesterol alters lipid raft structure and function regulating neutrophil Ca^{2+} entry and respiratory burst: Correlations with calcium channel raft trafficking. *J Immunol*. 2007;178:5253–5261.

Arteriosclerosis, Thrombosis, and Vascular Biology

JOURNAL OF THE AMERICAN HEART ASSOCIATION

Membrane Cholesterol Is a Biomechanical Regulator of Neutrophil Adhesion

Hana Oh, Emile R. Mohler III, Aiwei Tian, Tobias Baumgart and Scott L. Diamond

Arterioscler Thromb Vasc Biol. 2009;29:1290-1297; originally published online August 10, 2009;
doi: 10.1161/ATVBAHA.109.189571
Arteriosclerosis, Thrombosis, and Vascular Biology is published by the American Heart Association, 7272 Greenville Avenue, Dallas, TX 75231

Print ISSN: 1079-5642. Online ISSN: 1524-4636

Supplement Material

Membrane cholesterol is a biomechanical regulator of neutrophil adhesion.

Running Title: Oh et al. Cholesterol alters neutrophil rolling and adhesion.

Hana Oh[1], Emile R. Mohler III[2], Aiwei Tian[1,3], Tobias Baumgart[3] and Scott L. Diamond[1]*

[1]Department of Chemical and Biomolecular Engineering
Institute for Medicine and Engineering
University of Pennsylvania

[2]Department of Medicine
University of Pennsylvania

[3]Department of Chemistry
University of Pennsylvania

1024 Vagelos Research Laboratory
3340 Smith Walk
Philadelphia, PA 19104
Tel.: (215)573-5702
Fax: (215)573-6815
sld@seas.upenn.edu

SUPPLEMENTAL MATERIALS

Materials and cell culture

Human serum albumin (HSA; Golden West Biologicals), Hank's Balanced Salt Solution (HBSS; Invitrogen) without Ca^{2+}, Mg^{2+}, or phenol red, and methyl-β-cyclodextrin (MβCD) were stored according to manufacturers' instructions. Cholesterol (Sigma) was dissolved in a chloroform:methanol solution (1:1 by vol.) for storage. N-formyl-L-methionyl-L-leucyl-L-

phenylalanine (fMLP; Calbiochem) and Interleukin-1 (IL-1; BioLegend) were used to activate neutrophils and endothelial cells, respectively.

Human promyelocytic leukemia (HL-60) cells were cultured in RPMI1640 medium with sodium bicarbonate and L-glutamine (Invitrogen) supplemented with 5% fetal bovine serum according to manufacturer's instructions. Cells were incubated at 37°C in 5% CO_2 and subcultured to 5 x 10^5/mL every 3 days. Cells were induced with dimethyl sulfoxide (DMSO) to differentiate to mature granulocytes as previously described (1).

Human aortic endothelial cells (HAEC) were maintained in EGM-2 medium with supplements (Lonza), according to manufacturer's instructions (final serum concentration: 2%). Glass slides (38 x 75 mm) were coated with type 1 collagen (BD Biosciences) at 50 µg/mL in 0.02 N acetic acid. For flow chamber experiments, cells were seeded on at a density of 1 to 2×10^6 cells per slide and cultured to confluency.

Isolation of neutrophils

Human blood was obtained via venipuncture from healthy adult donors who had not taken any medications or consumed any alcohol in the prior 72 hours and from hypercholesterolemic (HC) patients (plasma cholesterol >300 mg/dL) in accordance with Institutional Review Board approval. Neutrophils were isolated by centrifugation with Lympholyte®-poly separation medium (Cedarlane Laboratories) as previously described (2). Neutrophils were counted and diluted with a 2% solution of human serum albumin (HSA) in Hank's Balanced Salt Solution (HBSS) with Ca^{2+} to a final concentration of 1 to 2 x 10^6 cells/mL.

Flow Cytometry

Isolated neutrophils at 10^6 cells/mL in HBSS/Ca/Mg/HSA were incubated with FITC-anti-CD11b or FITC-anti-CD18 (Ancell). Samples were incubated for 30 min at room temperature in the dark, washed and diluted in 1% formaldehyde solution in PBS, and immediately run on the cytometer (FACSCalibur, Becton-Dickinson) at10,000 events/sample. Neutrophils were identified by forward and side scatter properties in accordance to established criteria (3).

Quantification of cholesterol level

The amount of cholesterol was quantified using the Amplex Red® assay (Molecular Probes). Briefly, cell samples were washed once in PBS and resuspended in the Amplex Red® reaction buffer (0.1 M potassium phosphate, 0.05 M NaCl, 5 mM cholic acid, 0.1% Triton X-100, pH 7.4) at a concentration of 10^6 cells/mL and vortexed. Resulting cell lysates were pipetted in 50-µL aliquots into a 96-well tissue culture plate (Falcon/Becton Dickinson), and 50 µL of Amplex Red working solution (300 µM Amplex Red® reagent, 2 U/mL horseradish peroxidase, 2 U/mL cholesterol oxidase, and 0.2 U/mL cholesterol esterase) was added to each well. After a 40 minute-incubation at 37°C, fluorescence was measured on a CytoFluor II fluorescent plate reader (PerSeptive Biosystems) at an excitation wavelength of 530 nm and an emission wavelength of 590 nm.

Flow Chamber imaging and video analysis

Data were recorded using a JVC Professional Series VCR Super VHS and Sony Trinitron connected to the CPU/microscope/image processor system. Images were captured at 28 frames per second (fps) and analyzed frame-by-frame using the JVC VHS and Adobe Premier Elements® software. For high-speed imaging, images were captured using a Motion-Corder Analyzer high-speed digital camera (Eastman Kodak, Rochester, NY) at an imaging rate of 240

fps and analyzed frame-by-frame. ImageTool (UTHSCSA, Version 2.00) software was used to transfer images from the videotape onto the CPU. Scion Image and ImageJ (NIH) software plugins were used to analyze cell trajectories and membrane tether lengths. For HAEC flow chambers, each field of view (FOV, 0.1 mm^2) of neutrophils flowing over HAEC was recorded in 10-sec video segments. Scion Image and ImageJ (NIH) software was used to analyze trajectories of neutrophils and membrane tether lengths. ParticleTracker and MultiTracker plugins in ImageJ were used to obtain rolling length, velocity, and firm arrest data

Flow chamber shear rate calculations

Shear rates in the flow chambers were determined from the Navier-Stokes equation for laminar flow of a Newtonian fluid: $\tau_w = 6Q\mu/B^2W$. The wall shear rate, γ_w (sec^{-1}), was calculated as $\gamma_w = 6Q/B^2W$. In these equations, Q represents the flow rate (cm^3/sec), μ is the viscosity (0.01 Poise at room temperature), B is the total plate separation of the rectangular flow chamber, and W represents the width of the chamber, where B = 0.02 cm and W = 0.2 cm for the microcapillary chamber and B = 0.025 cm and W = 2.5 cm for the HAEC flow chamber. Microcapillary studies were performed at a flow rate of 80 µL/min, corresponding to a venous shear stress of 1 dyne/cm^2 and a venous wall shear rate of 100 sec^{-1}.

Whole-cell deformation assay parameters

For the whole-cell deformation assay, we analyzed the videomicroscopy data frame by frame, with t = 0 msec defined as 2 frames (about 8 msec) before contact. To quantitatively compare the degree of deformation, we tracked the centroid location (x,y) of the cells and measured *d*, the distance between the centroids, while cells were in contact with the bead at angle θ. For two hard spheres during collision, this distance would remain identical throughout contact, which would equal the sum of the radius of the cell and the radius of the bead: d_0 = 9 µm. We

calculated the difference between these two values as $R = d - d_0$, which defines $R = 0$ for two nondeformable spheres, and tracked them during contact. *Average contact lifetime* refers to the time between initial contact between the flowing cell and the bead; *maximum deformation* is the state at which the distance between the centroids (R) is the smallest; and *maximum contact area* is the contact area between the cell and the bead at this value of R.

FRAP (Fluorescence Recovery After Photobleaching) measurements

A 1 mL sample of isolated neutrophils was labeled with 5 µl of BSA-linked lipid analog dye DiIC12(3) for 10 min at room temperature, protected from light. Cells were washed with HBSS and transferred onto a glass coverslip. We used a dual micropipette setup with a motorized manipulator system (Luigs & Neumann, Germany) as previously described (4). Briefly, the 10-µm-diameter bead coated with anti-CD18 was aspirated with one micropipette at a suction pressure of about 60 Pa, while the labeled neutrophil was aspirated with the second micropipette at 5-10 Pa. We attached the bead briefly to the cell, then slowly pulled the bead away to extract a tether of about 10 µm.

A 5 µm region of the tether near the bead was bleached with the 543 nm, 488 nm, and 405 nm lasers at full power illumination. During fluorescence recovery, the excitation intensity of the 543 nm laser was decreased to 0.2% to 0.3% of full power. Cells were imaged by fluorescence confocal microscopy (Olympus FV300 and IX81), using a 60x, 1.2 NA water immersion objective (Olympus). Image analysis was performed using Matlab (Mathworks) and ImageJ (National Institutes of Health). Recovery and diffusion data were fitted with a one-dimensional diffusion model using the approach described (5).

Statistical Analysis

Statistical analysis of the data was performed using a standard two-sample Student's t-test assuming unequal variances of the two data sets. Statistical significance was determined using a two-tail distribution assumption and was set at 1% ($p<0.01$).

.

Supplemental Materials References

1. Hauert AB, Martinelli S, Marone C, Niggli V. Differentiated HL-60 cells are a valid model system for the analysis of human neutrophil migration and chemotaxis. *The International Journal of Biochemistry & Cell Biology*. 2002; 34:838-854.

2. Edmondson KE, Denney WS, Diamond SL. Neutrophil-bead collision assay: Pharmacologically induced changes in membrane mechanics regulate the PSGL-1/P-selectin adhesion lifetime. *Biophys J*. 2005; 89: 3603-3614.

3. van Eeden SF, Klut ME, Walker BAM, Hogg JC. The use of flow cytometry to measure neutrophil function. *J Immunol Methods*. 1999; 232: 23-43.

4. Tian A, Baumgart T. On the sorting of lipids and proteins in membrane curvature gradients. *Biophys J*. In press, 2009.

5. Daniels DR and Turner MS. Diffusion on membrane tubes: a highly discriminatory test of the Saffman-Delbruck theory. *Langmuir* 2007; 23(12): 6667-6670.